A 3-D Positioning Algorithm for AOA-Based VLP With an Aperture-Based Receiver

Heidi Steendam, *Senior Member, IEEE*

***Abstract*—We consider a visible light positioning system using modulated LEDs at the transmitter and photodiodes (PDs) combined with apertures at the receiver. The layout of the aperture-based receiver is designed in order to have angular diversity, implying it can detect the direction from which light is coming, by simply comparing the relative differences in received signal strength values in the different PDs. Hence, with this receiver, it is possible to extract the angle-of-arrival (AOA) of the light without needing the knowledge of the transmitted optical power. In this paper, we consider an algorithm, based on the maximum likelihood (ML) principle, to estimate the AOA, and obtain the position of the receiver in 3-D through triangulation. The ML algorithm, of which the practical implementation searches for the optimal value of the AOA starting from an initial estimate, suffers from convergence problems if the initial estimate is too far from the true AOA. Hence, we propose an initial low-complexity coarse estimation algorithm for the AOA, and make the algorithm iterative, where in each iteration, the initial estimate for the AOA is updated based on the previous position estimate. We show that the algorithm yields centimeter performance, i.e., an accuracy of 10 cm or better, using a limited number of LEDs, e.g., four LEDs for a 5 m × 5 m area.**

***Index Terms*—VLP, positioning, angle-of-arrival, maximum likelihood.**

I. Introduction

MANY applications require the knowledge of the user's position. However, the ubiquitous GPS technology can not provide accurate indoor position estimates. Hence, much research has been devoted to indoor positioning solutions since the beginning of this century. However, none of the approaches, e.g. WiFi, BLE or UWB, combines high accuracy with low cost and low power consumption. Recently, visible light positioning (VLP) received considerable attention [1]–[16].

Compared to other approaches, VLP has several advantages. Firstly, white LEDs are gradually replacing traditional light sources for lighting and can be modulated up to several MHz. As the VLP system can coexist with the lighting system, the installation and maintenance cost of the infrastructure is low. Further, not only white LEDs are widespread available, but also they are commonly attached to the ceiling at regular intervals to provide uniform lighting, implying most positions in a room will have a line-of-sight link with the LEDs. Secondly, visible light suffers less from multipath interference than RF approaches, and the light is blocked by opaque walls. Although the positioning accuracy will be affected by diffusion of the light, experiments showed that the accuracy that can be obtained is of the order of centimetres [3], [6], [7]. Thirdly, recent receivers for VLP employ photodiodes (PDs) to detect the light, resulting in a high energy efficiency. Finally, many RF solutions suffer from scalability issues, reducing the number of users that can simultaneously use the positioning system, as they require two-way communication to estimate the user's position. In contrast, the VLP system proposed in this paper can accurately estimate a position based on a broadcast optical signal, i.e. no communication from the user to the luminaire is required. As a result, a VLP positioning system can readily serve a large amount of users. Hence, the VLP approach must be considered as a viable solution for indoor positioning.

In most positioning systems, a two-stage approach is used, as direct estimation of a user's position from the received signal is often computationally too complex. In such a two-stage approach, position-related information is extracted from the received signal based on e.g. the time-of-arrival (TOA), the received signal strength (RSS) or the angle-of-arrival (AOA). In the second stage, the position is computed using trilateration or triangulation. Only a few works in the literature consider a TOA approach, e.g. [5], [10], as this TOA approach requires not only two-way communication, but also perfect synchronization between the transmitter and receiver. RSS-based approaches that estimate the distance between the LED and the receiver are far more popular [3], [4], [7]–[9], [11], [16]. In this approach, the distance is directly computed from the square-root of the RSS, followed by trilateration to compute the position. However, to determine this distance, the receiver needs to perfectly know the transmitted optical power, which is unrealistic in practice. Hence, although these papers report centimetre accuracy, not only through theoretical simulations but also with experiments, these experiments are done in controlled situations. In practice, the performance will rapidly degrade if the transmitted optical power is not perfectly known at the receiver. On the other hand, AOA-based approaches [6], [12]–[14], must be able to distinguish the direction from which the light is coming. This can be achieved by using a directional receiver, e.g. as in [6], [12], [17], and [18]. The complexity of the positioning

Manuscript received February 22, 2017; revised July 15, 2017; accepted September 16, 2017. Date of publication November 16, 2017; date of current version January 5, 2018. This work was supported in part by the Flemish Fund for Scientific Research and in part by the Interuniversity Attraction Poles Programme initiated by the Belgian Science Policy Office.

The author is with the Department of Telecommunications and Information Processing, Ghent University, 9000 Ghent, Belgium (e-mail: heidi.steendam@ugent.be).

Color versions of one or more of the figures in this paper are available online at http://ieeexplore.ieee.org.

Digital Object Identifier 10.1109/JSAC.2017.2774478

algorithm and the positioning performance that can be obtained with these systems is comparable. The only difference is the implementation of the directional receiver. In this paper, we focus on the receiver structure from [18], and consider the AOA approach to estimate the user's position.

The directional receiver structure from [18] consists of a number of receiving elements (REs), where each RE contains a PD and an aperture. The apertures are placed in such a way that the receiver exhibits angular diversity. The aperture-based receiver from [18] was originally proposed for optical MIMO communication, but we directly recognized its potential for VLP. For this receiver, the Cramer-Rao bound was investigated in [19] and [20] for direct estimation of the position, and later in [21] for AOA-based positioning. This Cramer-Rao bound serves as a benchmark to evaluate the optimality of position estimation algorithms, and can be used to optimize the parameters of the receiver layout. However, the papers [19]–[21] do not consider practical algorithms to estimate the user's position. In this paper, we propose a practical iterative algorithm to estimate the AOA between each RE and LED, and obtain the user's position in three dimensions (3D) using triangulation. The algorithm is based on the maximum-likelihood (ML) principle, and searches in each iteration for the optimal AOA, starting from an initial estimate of the AOA, for each LED–RE pair. To initialize the algorithm, we propose a low-complexity algorithm that produces coarse estimates for the AOAs. To improve the convergence of the algorithm, we update the AOAs after each ML step based on the position obtained with the triangulation step, and iterate until the position estimate has converged or a maximum number of iterations is reached. We show that the resulting iterative algorithm accurately estimates the position in 3D. Further, the performance of the algorithm is compared with the Cramer-Rao bound from [21]. When the iterative algorithm converges well, the mean squared error (MSE) on the position estimate approaches the Cramer-Rao bound.

The paper is organized as follows. In Section II, we describe the transmitter and receiver structure, and define the AOA. Next, in Section III, the positioning algorithm is considered. First, in Section III-A, we give a short overview of the triangulation algorithm. Then, in Section III-B, we describe the iterative ML algorithm, and finally, in Section III-C, we introduce the coarse estimators. In Section IV, we evaluate the performance of the proposed algorithm, and conclusions are given in Section V.

II. System Description

A. Transmitter

Let us consider a visible light positioning system where K white LEDs are attached to the ceiling. The LEDs, which are primarily used for lighting, are placed at positions $(x_{S,i}, y_{S,i}, z_{S,i})$, point downwards and can be modelled as Lambertian LEDs with order m_i, $i = 1, \ldots, K$. To be able to distinguish the light broadcast by the different LEDs, each LED transmits a different signal $s_i(t)$, $i = 1, \ldots, K$. We assume the signal transmitted by LED i is a dc-biased windowed sinusoid waveform with duration T:

$$s_i(t) = A_i w(t)(1 + \cos(2\pi f_{c,i} t)), \tag{1}$$

where the frequencies $f_{c,i}$, $i = 1, \ldots, K$ are selected to have an integer number of periods over the interval $[0, T]$, i.e. $f_{c,i}T$ is integer. Further, we assume the frequencies $f_{c,i}$ are orthogonal over the interval $[0, T]$, i.e. $(f_{c,i} - f_{c,i'})T$, $i, i' = 1, \ldots, K$ is integer. To avoid annoying flicker that is visible by the human eye, the frequencies $f_{c,i}$ must be sufficiently large, e.g., $f_{c,i} > 1$ kHz. The window function $w(t)$ is selected as a rectangular window function in the interval $[0, T]$. This case corresponds to the selection of the signals according to a dc-biased orthogonal frequency division multiplexing (OFDM) signal [22]. Other window functions are also possible, resulting in slightly different received signal strength values. Although the choice of the window function will influence the positioning performance, its effect will be rather small.

B. Receiver

To detect the light transmitted by the different LEDs, we consider the receiver introduced in [18]. This receiver consists of M receiving elements (REs), where each RE contains a photodiode (PD) and an aperture. The M PDs are arranged in the same plane, and we assume they are circular with radius R_D. The apertures consist of circular holes with radius R_D in an opaque screen that is placed parallel to the plane of the PDs, at a height h_A above this plane. Further, we assume that the only light that reaches PD j is the light that passes through aperture j. We suppose the radius R_D of the apertures is large compared to the wavelength of the light, so diffraction effects can be ignored, and the light that passes through the aperture will introduce a circular light spot with radius R_D on the plane of the PDs.

We assume the receiver is placed parallel to the ceiling. However, extension of the results to other orientations of the receiver is straightforward, provided the receiver knows its orientation. This orientation can easily be obtained using the sensors of an inertial measurement unit (IMU), which is commonly available in many mobile devices. Our goal is to estimate the position of the receiver. To this end, we select a reference position (x_U, y_U, z_U) in the plane of the apertures (see Fig. 1). The positions of the apertures are given by $(x_{AP,j}, y_{AP,j}, z_{AP,j}) = (x_U + \delta x_j, y_U + \delta y_j, z_U)$. In this paper, we assume the apertures are uniformly distributed over a circle with as centre the reference position, i.e. $(\delta x_j, \delta y_j) = (\epsilon \cos\ (j-1)\frac{\pi}{M}, \epsilon \sin\ (j-1)\frac{\pi}{M})$ with $\epsilon = 5\ R_D$, as shown in Fig. 1(b). However, from simulations in [20], it was noted that the placement of the apertures has a negligible effect on the performance as long as the assumption, that the only light that reaches a PD is the light that comes through its aperture, is fulfilled. In order to change the field-of-view of RE j, we slightly displace the PD with respect to its aperture. Defining the displacement $(x_{PD,j}, y_{PD,j}) = (d_{PD,j} \cos \psi_{PD,j}, d_{PD,j} \sin \psi_{PD,j})$, the position of the centre of PD j can be written as $(x_{AP,j} + x_{PD,j}, y_{AP,j} + y_{PD,j}, z_U - h_A)$. The parameters h_A, $d_{PD,j}$ and $\psi_{PD,j}$ have a large

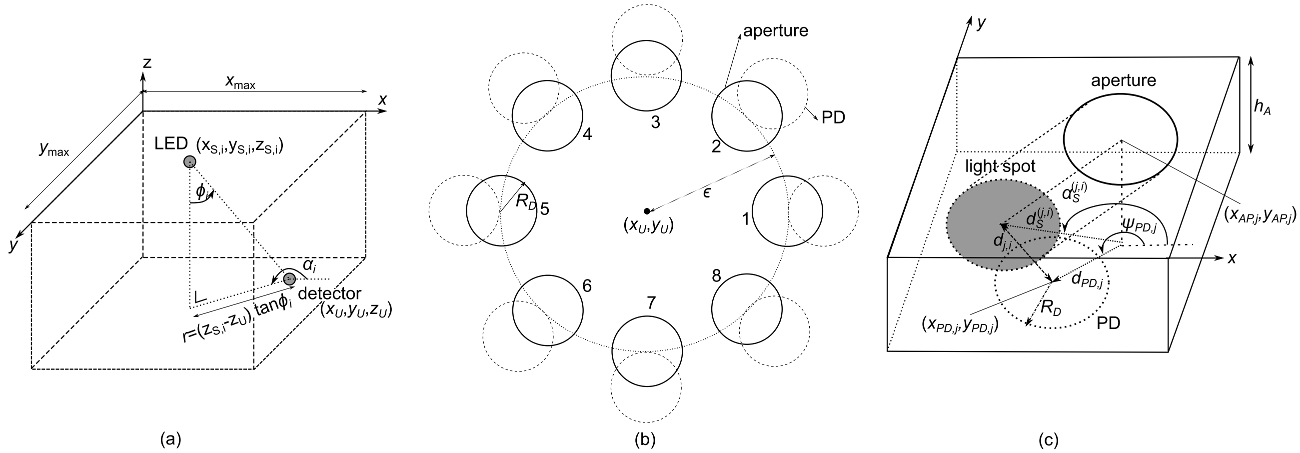

Fig. 1. a) Definition of the incident and polar angles (ϕ, α), b) top view of the receiver with 8 REs, and c) one RE.

TABLE I
OVERVIEW OF THE PARAMETERS OF THE RECEIVER

Name	Description
M	number of REs
$\boldsymbol{\rho} = (x_U, y_U, z_U)$	reference position on receiver
R_D	radius of PD and aperture
h_A	distance between plane of PDs and plane of apertures
$(x_{AP,j}, y_{AP,j}, z_{AP,j})$	coordinates of center of aperture j with $(x_{AP,j}, y_{AP,j}, z_{AP,j}) = (x_U + \delta x_j, y_U + \delta y_j, z_U)$
$(\delta x_j, \delta y_j)$	x/y distance of center of aperture j to reference position $\boldsymbol{\rho}$ with $(\delta x_j, \delta y_j) = \epsilon(\cos\frac{(j-1)\pi}{M}, \sin\frac{(j-1)\pi}{M})$, $j = 1, \ldots, M$, $\epsilon = 5R_D$
$(x_{PD,j}, y_{PD,j})$	displacement of PD j w.r.t. its aperture with $(x_{PD,j}, y_{PD,j}) = d_{PD,j}(\cos\psi_{PD,j}, \sin\psi_{PD,j})$

influence on the field-of-view of the receiver. To obtain a receiver that has a large field-of-view, the displacement of the PDs must be symmetrical, i.e. $\psi_{PD,j}$ is preferably uniformly distributed over the interval $[0, 2\pi[$, and $d_{PD,j}$ may not be too large. Therefore, we select $\psi_{PD,j} = (j-1)\frac{\pi}{M}$ and $d_{PD,j} = d_{PD}$. Further, to have a receiver that can detect the direction from which light is coming, d_{PD} must be sufficiently large. In [20], it is shown that the optimal value for d_{PD} is in the interval $[0.5R_D, 1.5R_D]$. The parameters of the receiver are summarized in Table I.

The reference position (x_U, y_U, z_U) of the receiver will be estimated based on the AOAs between the receiver and the different LEDs. We define the incident angle ϕ_i and the polar angle α_i between the i-th LED and the reference point on the receiver as:

$$\begin{aligned} x_{S,i} - x_U &= (z_{S,i} - z_U)\tan\phi_i \cos\alpha_i \\ y_{S,i} - y_U &= (z_{S,i} - z_U)\tan\phi_i \sin\alpha_i. \end{aligned} \tag{2}$$

Each RE will capture light from the different LEDs. In order to extract the angles (ϕ_i, α_i), the receiver must be able to separate the contributions from the different LEDs. To this end, the output of each PD is correlated with the signals $\zeta_i(t) = w(t)\cos(2\pi f_{c,i} t)$, $i = 1, \ldots, K$. This correlation will remove the dc contribution from the PD output. This is necessary as the dc component suffers from interference, i.e. all LEDs contribute to the dc component, so using this dc component would reduce the positioning accuracy. Further, due to the orthogonality of the frequencies $f_{c,i}$, the correlation of a PD output with $\zeta_i(t)$ will contain the contribution from LED i only. This yields the vector of observations $\mathbf{r} = (\mathbf{r}_1^T \ldots \mathbf{r}_M^T)^T$ where

$$\mathbf{r}_j = (r_{j,1} \ldots r_{j,K})^T \tag{3}$$

and

$$r_{j,i} = R_p h_c^{(j,i)} s_i + n_{j,i}. \tag{4}$$

In (4), R_p is the responsitivity of the PD, $s_i = \int_0^T \zeta_i(t) s_i(t) dt = A_i T/2$, $n_{j,i} = \int_0^T \zeta_i(t) n_j(t) dt$ is the contribution of the shot noise $n_j(t)$ from PD j, and $h_c^{(j,i)}$ is the channel gain from LED i to PD j. The shot noise can be modelled as a zero-mean Gaussian random variable with covariance $E[n_{j,i} n_{j',i'}] = \frac{N_0 T}{2}\delta_{i,i'}\delta_{j,j'}$ with $N_0 = 2\, q R_p p_n A_D \Delta\lambda$ [23], where q is the charge of an electron, R_p the responsitivity of the PD, p_n the background spectral irradiance, A_D the area of the PD and $\Delta\lambda$ the bandwidth of the optical filter placed in front of the PD. The channel gain $h_c^{(j,i)}$ is given by [23]:

$$h_c^{(j,i)} = \frac{m_i + 1}{2\pi (z_{S,i} - z_U)^2} A_0^{(j,i)} \cos^{m_i+3}\phi_{j,i}, \tag{5}$$

where $A_0^{(j,i)}$ is the overlap area between PD j and the light spot coming from LED i, and $\phi_{j,i}$ is the incident angle of the light coming from LED i at aperture j, with

$$\begin{aligned} x_{S,i} - x_{AP,j} &= (z_{S,i} - z_{AP,j}) \tan\phi_{j,i} \cos\alpha_{j,i} \\ y_{S,i} - y_{AP,j} &= (z_{S,i} - z_{AP,j}) \tan\phi_{j,i} \sin\alpha_{j,i}. \end{aligned} \tag{6}$$

The overlap area $A_0^{(j,i)}$ is determined by the distance $d_{j,i}$ (see Fig. 1(c)) between the centres of the light spot and the PD, i.e.

$$A_0^{(j,i)} = \begin{cases} 2R_D^2 \arccos\left(\dfrac{d_{j,i}}{2R_D}\right) & 0 \le d_{j,i} \le 2R_D \\ \quad - \dfrac{d_{j,i}}{2}\sqrt{4R_D^2 - d_{j,i}^2} & \\ 0 & d_{j,i} > 2R_D. \end{cases} \tag{7}$$

Defining

$$\begin{aligned} \Delta x &= x_{PD,j} - d_S^{(j,i)} \cos\alpha_S^{(j,i)} \\ \Delta y &= y_{PD,j} - d_S^{(j,i)} \sin\alpha_S^{(j,i)}, \end{aligned} \tag{8}$$

with $d_S^{(j,i)} = h_A \tan\phi_{j,i}$ and $\alpha_S^{(j,i)} = \pi + \alpha_{j,i}$, the distance $d_{j,i}$ can be written as

$$d_{j,i} = \sqrt{\Delta x^2 + \Delta y^2}. \tag{9}$$

III. Positioning Algorithm

A. Triangulation

In the algorithm that will be proposed in this paper, the AOAs (ϕ_i, α_i) between the receiver and the different LEDs will be estimated. To obtain the position of the receiver based on these AOA estimates, triangulation is used. In this triangulation algorithm, we construct a set of linear equations in (x_U, y_U, z_U), where each LED will contribute to maximum two equations, depending on the reliability of the estimates of ϕ_i and α_i. Taking into account (2), if for LED i a reliable estimate for both ϕ_i and α_i is available, LED i will contribute to two equations:

$$\begin{aligned} x_U - z_U \tan\phi_i \cos\alpha_i &= x_{S,i} - z_{S,i} \tan\phi_i \cos\alpha_i \\ y_U - z_U \tan\phi_i \sin\alpha_i &= y_{S,i} - z_{S,i} \tan\phi_i \sin\alpha_i, \end{aligned} \tag{10}$$

while if only a reliable estimate for α_i is available, LED i will contribute to one equation:

$$x_U \sin\alpha_i - y_U \cos\alpha_i = x_{S,i} \sin\alpha_i - y_{S,i} \cos\alpha_i. \tag{11}$$

This will occur if the incident angle ϕ_i is larger than the maximum incident angle that can be estimated with the coarse estimator. When the estimates of both ϕ_i and α_i are not reliable, because LED i is out of the field-of-view of the receiver, LED i will not contribute to the set of equations. Combining the equations for the different LEDs, we obtain the following expression in matrix notation:

$$\mathbf{A}\boldsymbol{\rho} = \mathbf{b}, \tag{12}$$

where the matrix $\mathbf{A}$ and the vector $\mathbf{b}$ collect the contributions from the linear equations (10) and (11), and $\boldsymbol{\rho} = (x_U, y_U, z_U)$ if we have for at least one LED a reliable estimate of ϕ_i, while $\boldsymbol{\rho} = (x_U, y_U)$ if for none of the LEDs, the estimate of ϕ_i is reliable. In this latter case, the triangulation algorithm will not be able to return an estimate of the height z_U of the receiver. Taking into account (12), the least square (LS) estimate $\hat{\boldsymbol{\rho}}_{LS}$ of $\boldsymbol{\rho}$ is given by

$$\hat{\boldsymbol{\rho}}_{LS} = (\mathbf{A}^T\mathbf{A})^{-1}\mathbf{A}^T\mathbf{b}. \tag{13}$$

B. Iterative ML-Based Estimation

The core of the proposed iterative algorithm is the ML estimator. Taking into account that the additive noise in (4) is a Gaussian random variable, the ML estimate of $\boldsymbol{\theta} = (\boldsymbol{\phi}\ \boldsymbol{\alpha})$, with $\boldsymbol{\phi} = (\phi_1 \dots \phi_K)$ and $\boldsymbol{\alpha} = (\alpha_1 \dots \alpha_K)$, reduces to [24]

$$\hat{\boldsymbol{\theta}}_{ML} = \arg\min_{\boldsymbol{\theta}} ||\mathbf{r} - R_p \mathbf{H}_c \mathbf{s}||^2 \tag{14}$$

where $||\cdot||^2$ is the Euclidean norm, $(\mathbf{H}_c)_{j,i} = h_c^{(j,i)}$ and $\mathbf{s} = (s_1 \dots s_K)$. The cost function $||\mathbf{r} - R_p \mathbf{H}_c \mathbf{s}||^2$ in (14) is a highly non-linear function of $\boldsymbol{\theta}$, and a closed-form solution for this estimate is not available. However, several practical algorithms to solve (14) exist. In these algorithms, the algorithm starts from an initial estimate for $\boldsymbol{\theta}$ and z_U, and searches for the solution $\hat{\boldsymbol{\theta}}_{ML}$ that optimizes the cost function. The convergence of the algorithms depends on the accuracy of the initial estimates. Especially if the initial estimate of z_U is far from the true value of z_U, the estimate $\hat{\boldsymbol{\rho}} = (\hat{x}_U, \hat{y}_U, \hat{z}_U)$ of the position, obtained with the ML AOA estimation algorithm followed by the triangulation algorithm, will not always converge to the true position $\boldsymbol{\rho} = (x_U, y_U, z_U)$. To improve the convergence of the position estimation, we consider an iterative approach.

In this iterative algorithm, we first estimate the AOA $\hat{\boldsymbol{\theta}}$ using the ML algorithm, and subsequently the position $\boldsymbol{\rho}$ with the triangulation algorithm. The resulting position estimate $\hat{\boldsymbol{\rho}}$ is then used to update the AOA with (2). The estimate $\hat{z}_U$ and the updated AOA are applied to the ML algorithm in the next iteration. This operation is repeated until the algorithm has converged, i.e. the Euclidean distance between successive estimates of the position is below a threshold, or the maximum number of iterations is reached. An overview of the iterative algorithm is shown in Table II. In our simulations, we stop iterating when the Euclidean distance between successive position estimates is smaller than the threshold, which is set to 1 mm in our simulations, i.e. $||\hat{\boldsymbol{\rho}}^{(\ell)} - \hat{\boldsymbol{\rho}}^{(\ell-1)}||^2 < 10^{-6}\ \mathrm{m}^2$. If the initial estimate on the AOA is reliable, we noticed in our simulations that only a limited number of iterations was needed. However, if the initial estimate of the AOA is not reliable, in some cases the iterative algorithm diverges, i.e. the Euclidean distance between successive position estimates $\hat{\boldsymbol{\rho}}^{(\ell)}$ grows. In that case, the algorithm is stopped, and a message is returned that the position could not be determined. This does not occur systematically: in a next time instant, for the same position but with different noise values, the algorithm might converge. In other cases, if the initial AOA estimate is not reliable, the algorithm will converge, although very slowly. Hence, the Euclidean distance between successive position estimates $\hat{\boldsymbol{\rho}}^{(\ell)}$ decreases, but will not go below the threshold unless a large number of iterations is allowed. To avoid the increase in complexity and the risk that the algorithm goes into an infinite loop, we stop the algorithm after a maximum

TABLE II
ITERATIVE ALGORITHM

initial coarse estimation of $\boldsymbol{\theta}^{(0)}$ (see Sec. III-C)
triangulation: estimate $\hat{\boldsymbol{\rho}}^{(0)}$
update $\boldsymbol{\theta}^{(0)}$ using (2) and $\hat{\boldsymbol{\rho}}^{(0)}$
for $\ell = 1$: maxiterations **do**
    ML estimation $\boldsymbol{\theta}^{(\ell)}$ with as input $\boldsymbol{\theta}^{(\ell-1)}$ and $z_U^{(\ell-1)}$
    triangulation: estimate $\hat{\boldsymbol{\rho}}^{(\ell)}$
    update $\boldsymbol{\theta}^{(\ell)}$ using (2) and $\hat{\boldsymbol{\rho}}^{(\ell)}$
    if $||\hat{\boldsymbol{\rho}}^{(\ell)} - \hat{\boldsymbol{\rho}}^{(\ell-1)}||^2 <$ threshold **then**
        $\ell =$ maxiterations$+1$
    end if
end for

number of iterations. In our simulations, we set the maximum number of iterations to $maxiterations = 10$. The Euclidean distance between the successive estimates gives an indication about the reliability of the estimate.

C. Initial Coarse AOA Estimation

The iterative algorithm needs sufficiently accurate initial estimates of the AOA $\boldsymbol{\theta}$ and the height z_U in order to converge. To obtain a coarse estimate for the AOA, we take a closer look at the RSS values in the different PDs corresponding to a given LED i. For the receiver layout as shown in Fig. 1(b), the three largest values of the RSS normally occur in three adjacent REs, with the maximum RSS value in the middle RE, i.e. at indices $j_{\max} - 1$, $j_{\max}$ and $j_{\max} + 1$, where

$$j_{\max} = \arg\max_j \, r_{j,i}. \tag{15}$$

When this is the case, we consider the RSS measurements corresponding to LED i as reliable. On the other hand, if the three largest RSS values for LED i are not in adjacent REs, we can distinguish two cases. In the first case, the LED is just above the receiver, implying all RSS values are approximately the same. As in this case, LED i probably will also be the nearest LED, these RSS values will be larger than for most other LEDs (depending on the transmitted optical powers of the LEDs). In that case, the LED is considered as reliable and we set $\hat{\phi}_i^{(0)} = 0$, while α_i is not defined. However, when $\phi_i = 0$, the definition of α_i is not required to have the LED included in the triangulation. In the second case, when the LEDs are not approximately the same, the RSS measurements are noise dominated, and the RSS values are typically smaller than for other LEDs. This case corresponds to a LED that is out of the field-of-view of the receiver. Assuming $d_{PD,j} = d_{PD}$ and taking into account (8), the incident angle ϕ_i in that case will exceed $\phi_{out} \approx \text{atan}\frac{2R_D + d_{PD}}{h_A}$. This angle ϕ_{out} determines the radius d_{out} within which the receiver can see the LED, i.e. $d_{out} = (z_{S,i} - z_U)\tan\phi_{out}$. As a result, we are not able to find reliable coarse estimates for ϕ_i and α_i when $\phi_i \geq \phi_{out}$, and we will neglect this LED in the triangulation phase. In the remainder of this section, we will discuss the coarse estimation of ϕ_i and α_i for the case where the three largest RSS values are observed in adjacent REs, i.e. when $0 < \phi_i < \phi_{out}$. An overview of the parameters used in the coarse estimators is given in Table III.

1) Coarse Estimate of α_i: An indication of the polar angle α_i can be extracted from the RE that has the largest contribution from LED i. This RE yields the largest overlap

TABLE III
OVERVIEW OF PARAMETERS USED IN THE COARSE ESTIMATORS, $|j|_M$ IS j MODULO M

$j_{\max} = \arg\max_j r_{j,i}$	index of RE with maximum RSS value
$r_{\max,i} = r_{j_{\max},i}$	maximum RSS value
$\gamma_j = \frac{r_{j,i}}{r_{\max,i}}$	ratio of RSS values
$j_{opp} = \lvert j_{\max} + \frac{M}{2}\rvert_M$	index of RE opposite to $j_{\max}$
$\gamma_{opp} = \gamma_{j_{opp}}$	ratio of RSS values in RE j_{opp}
$\phi_{out} = \text{atan}\,\frac{2R_D+d_{PD}}{h_A}$	angle determining FOV of receiver
$d_{out} = (z_{S,i} - z_U)\tan\phi_{out}$	radius determining FOV of receiver
$\phi_{\max} = \text{atan}\,\frac{2R_D-d_{PD}}{h_A}$	maximum range coarse estimator
$d_{\max} = (z_{S,i} - z_U)\tan\phi_{\max}$	radius coarse estimator

between the light spot from LED i and the PD. Defining the index $j_{\max}$ as the index of the PD where the maximum RSS value occurs (15), it follows that

$$|\alpha_S^{(j,i)} - \psi_{AP,j_{\max}}|_{2\pi} = \min_j |\alpha_S^{(j,i)} - \psi_{AP,j}|_{2\pi}, \tag{16}$$

where $|\cdot|_{2\pi}$ is the absolute value of the argument modulo-2π with as range of outcomes the interval $[0, \pi]$. Hence, the difference in angle between $\alpha_S^{(j,i)}$ and $\psi_{AP,j_{\max}}$ is the smallest, indicating a coarse estimate for α_i can be obtained by taking into account $\alpha_S^{(j,i)} = \alpha_{j,i} + \pi$ and $\alpha_{j,i} \approx \alpha_i$[1]:

$$\hat{\alpha}_i = \psi_{AP,j_{\max}} + \pi. \tag{17}$$

However, in this case, $\hat{\alpha}_i$ can only take M values. Because the granularity of this estimate is large, this coarse estimate of α_i is often not sufficient for the ML algorithm to converge.

To improve the accuracy of the initial estimate of α_i, we define the function $RSS_i(\alpha)$ that is continuous in α, and takes the values $RSS_i(\psi_{AP,j} + \pi) = r_{j,i}$. With this function, we are able to interpolate between the M values of $\psi_{AP,j_{\max}}$. In a reliable RE, this function behaves nicely near the single maximum. To find the maximum of the function $RSS_i(\alpha)$, we approximate $RSS_i(\alpha)$ as a quadratic function:

$$RSS_i(\alpha) = a\alpha^2 + b\alpha + c, \tag{18}$$

where a, b and c are determined by $RSS_i(\psi_{AP,j} + \pi) = r_{j,i}$, $j \in \{j_{\max}, j_{\max} \pm 1\}$. Based on this quadratic function, we compute the value α that maximizes this quadratic function to obtain a coarse estimate for α_i:

$$\hat{\alpha}_i = \arg\max_\alpha \, RSS_i(\alpha) = -\frac{b}{2a}. \tag{19}$$

2) Coarse Estimate of ϕ_i: To obtain an estimate of ϕ_i, we take a closer look at the RSS values at the outputs of the PDs. Let us define the ratio $\gamma_j = \frac{r_{j,i}}{r_{\max,i}}$, $j = 1, \ldots, M$, where $r_{\max,i} = r_{j_{\max},i}$. This ratio γ_j of RE j is a function of both the incident angle ϕ_i and polar angle α_i. To find a coarse estimator for ϕ_i that can estimate ϕ_i without having the knowledge of α_i, we prefer a ratio γ_j that is essentially independent of ϕ_i. In Fig. 2, we plot the ratio γ_j as function

[1]From (2) and (6), it follows that when $\phi_i > 0$ and the dimensions of the receiver are small compared to the vertical distance between the LED and the receiver, i.e. $x_{AP,j}, y_{AP,j}, x_{PD,j}, y_{PD,j}$ and $h_A \ll (z_{S,i} - z_U)$, the angles $\phi_{j,i}$ and $\alpha_{j,i}$, $j = 1, \ldots, M$ are approximately equal, i.e. $\phi_{j,i} \approx \phi_i$ and $\alpha_{j,i} \approx \alpha_i$.

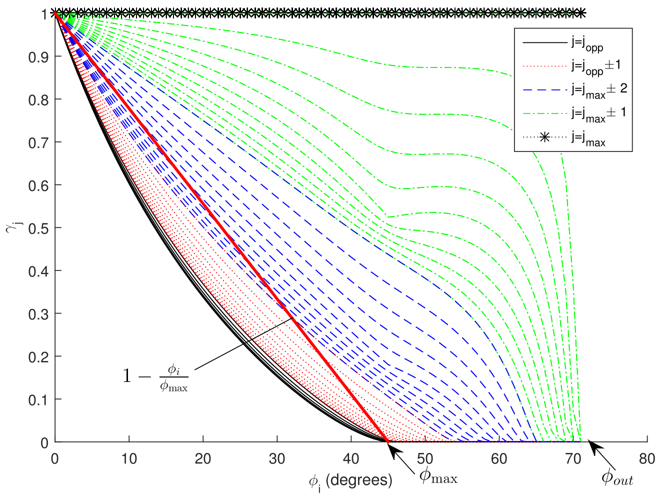

(a)

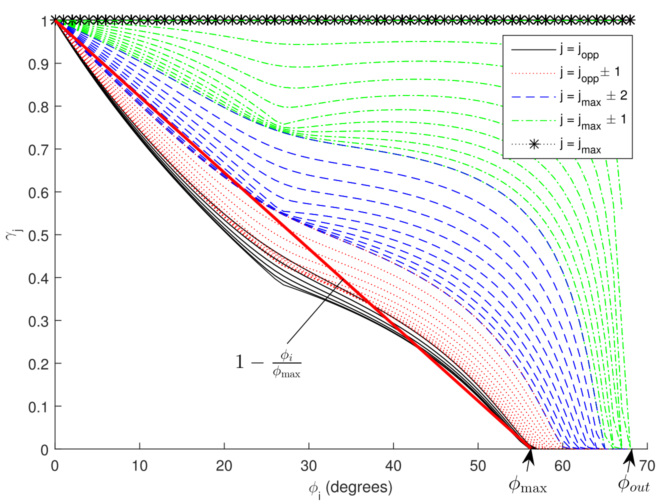

(b)

Fig. 2. The ratio γ_j as a function of the incident angle ϕ_i for $M = 8$, $d_{AP} = 5\ R_D$ and $h_A = R_D$. The angle $\phi_{\max} = 56.31°$. (a) $d_{PD} = R_D$ so $\phi_{\max} = 45°$ and $\phi_{out} = 71.6°$ (b) $d_{PD} = 0.5\ R_D$ so $\phi_{\max} = 56.3°$ and $\phi_{out} = 68.2°$.

of ϕ_i for $M = 8$, assuming no shot noise is present. Different lines with the same colour correspond to different values of α_i, i.e. $\alpha_i = -\frac{\pi}{8} + \frac{k}{10} \cdot \frac{\pi}{4}$, $k = 0, \ldots, 10$. Note that, due to the symmetry of the receiver, the ratios $\gamma_{j_{\max}+1}$ and $\gamma_{j_{\max}-1}$, i.e. the REs right next left and right of the RE with maximum RSS value, will show the same behaviour, similarly as the ratios $\gamma_{j_{\max}+2}$ and $\gamma_{j_{\max}-2}$, and the ratios $\gamma_{j_{opp}+1}$ and $\gamma_{j_{opp}-1}$. In the figure, it can be observed that the ratio γ_j is essentially independent of α_i when $j = j_{opp}$, i.e. for the RE opposite to the RE with the maximum RSS value, while the ratio γ_j depends more on α_i for other REs. Hence, the ratio $\gamma_{opp} = \gamma_{j_{opp}}$ is suitable to obtain a coarse estimate for ϕ_i without needing to know the value of α_i. The ratio γ_{opp} becomes zero for incident angles $\phi_i > \phi_{\max}$. This angle $\phi_{\max}$ corresponds to the incident angle above which RE j_{opp} no longer detects light from a LED. Taking into account (8), $\phi_{\max} \approx \mathrm{atan}\frac{2R_D - d_{PD}}{h_A}$.

A very simple estimator consists of approximating the ratio γ_{opp} as a linear function of ϕ_i:

$$\gamma_{opp} \approx 1 - \frac{\phi_i}{\phi_{\max}}, \tag{20}$$

from which follows that a coarse estimate for ϕ_i is obtained as

$$\hat{\phi}_i = \phi_{\max}(1 - \gamma_{opp}). \tag{21}$$

This approximation is illustrated in Fig. 2. With this coarse estimator, estimates of ϕ_i are restricted to the interval $[0, \phi_{\max}]$ and the radius within which the receiver is able to deliver an estimate of ϕ_i equals $d_{\max} = (z_{S,i} - z_U) \tan \phi_{\max}$. Examining Fig. 2, we observe that this simple approximation is better for $d_{PD} = 0.5R_D$ than for $d_{PD} = R_D$. Further, although the radius within which the receiver can see the LED is slightly larger for $d_{PD} = R_D$, i.e. $d_{out,d_{PD}=R_D} = 3h\frac{R_D}{h_A}$ while $d_{out,d_{PD}=0.5R_D} = 2.5h\frac{R_D}{h_A}$, the downside of the choice $d_{PD} = R_D$ is the much smaller radius within which the proposed coarse estimator for ϕ_i can deliver a reliable estimate for ϕ_i, i.e. $d_{\max,d_{PD}=0.5R_D} = 1.5\ h\frac{R_D}{h_A}$ while $d_{\max,d_{PD}=R_D} = h\frac{R_D}{h_A}$. As the larger field-of-view of the receiver with $d_{PD} = R_D$ does not outweigh the larger area in which the receiver with $d_{PD} = 0.5R_D$ can deliver a coarse estimate of ϕ_i, we select $d_{PD} = 0.5\ R_D$ in the remainder of the paper. We will show in the numerical results that for $d_{PD} = 0.5R_D$, the accuracy of the coarse estimator is sufficient for the iterative algorithm to converge.

Note that we assumed in the derivation of the algorithm that the RSS values are noiseless. In the presence of noise, the estimate of ϕ_i will be unreliable for small values of γ_{opp}, i.e. when $\phi_i \geq 0.9\phi_{\max}$. Therefore, we use this method to estimate ϕ_i only if the resulting $0 \leq \hat{\phi}_i < 0.9\phi_{\max}$. In all other cases, the coarse estimate of ϕ_i is considered as unreliable and will not be used in the triangulation phase, i.e. equation (11) is used instead of (10).

IV. Numerical Results

In this section, we evaluate the performance of the proposed estimator. We consider a receiver with $M = 8$ REs. As already mentioned in Section II, we select $(\delta x_j, \delta y_j) = (5R_D \cos\ (j-1)\frac{2\pi}{M}, 5R_D \sin\ (j-1)\frac{2\pi}{M})$, with $R_D = 1$ mm, and $(x_{PD,j}, y_{PD,j}) = (0.5R_D \cos\ (j-1)\frac{2\pi}{M}, 0.5\ R_D \sin\ (j-1)\frac{2\pi}{M})$. We assume the distance between the plane of the apertures and the plane of the PDs equals $h_A = R_D$, and the LEDs have Lambertian order $m = 1$. The level of the shot noise equals $N_0 = 8.4 \times 10^{-24}$ A^2/Hz, which corresponds to a background spectral irradiance $p_n = 5.8 \times 10^{-6}$ W/cm^2·nm [23], the responsitivity of the PD $R_p = 0.4$ mA/mW [25] and $\Delta\lambda = 360$ nm, for an optical filter placed in front of the PD that passes only visible light frequencies in the range 380 to 740 nm. Further, we consider the optical power of the LEDs equal to $A = 1$ W and a time interval $T = 10$ ms.

Let us first evaluate the performance of the coarse estimator. As in this coarse estimation step, not all angles ϕ_i and α_i can be obtained because of the limitations of the proposed coarse estimators, we consider the coarse estimation step from Section III-C, followed by a triangulation step. With

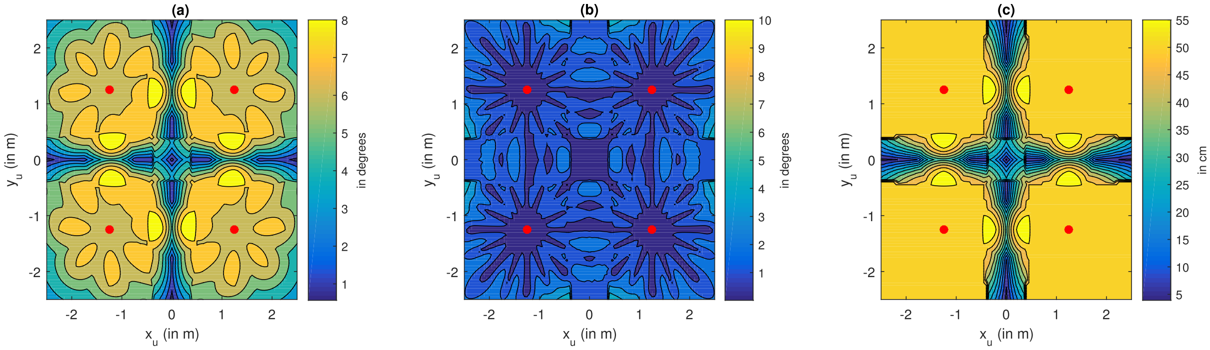

Fig. 3. rMSE of the coarse estimation for (a) ϕ_i (b) α_i (c) z_U as function of the position of the receiver in the room, for $A_i = 1$ W, $T = 0.01$ s, $M = 8$, $x_{\max} = y_{\max} = 5$ m, $R = 2.5$ m, $h = 2$ m.

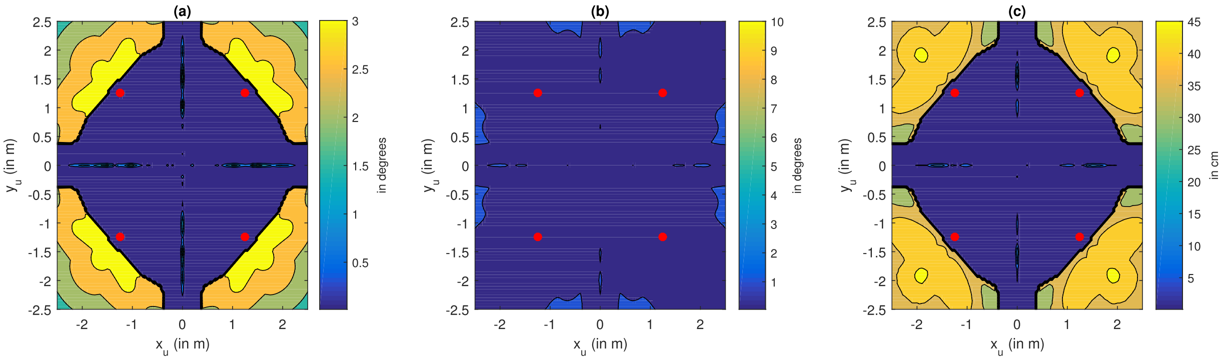

Fig. 4. rMSE of the ML step, no iterations for (a) ϕ_i (b) α_i (c) z_U as function of the position of the receiver in the room, for $A_i = 1$ W, $T = 0.01$ s, $M = 8$, $x_{\max} = y_{\max} = 5$ m, $R = 2.5$ m, $h = 2$ m.

the position estimate resulting from the triangulation step, we update the coarse estimates of ϕ_i and α_i using (2). We consider an area of 5 m×5 m, with four LEDs that are attached on the ceiling, i.e. $z_{S,i} = z_S = 0$ m, and that are arranged in a square around the centre of the area, with as spacing $R = 2.5$ m between the LEDs, i.e. $(x_{S,i}, y_{S,i}, z_{S,i}) = (\pm 1.25 \text{ m}, \pm 1.25 \text{ m}, 0 \text{ m})$. We assume the receiver is at a distance $h = -z_U = 2$ m below the ceiling. As mentioned in Section III-A, if no reliable estimates of ϕ_i, $i = 1, \ldots, 4$ are available for a position of the receiver, the triangulation step can not return a coarse estimate of z_U. In that case, we use as initial estimate $\hat{z}_U^{(0)} = -1.5$ m. We simulate the coarse estimation step followed by the triangulation step 100 times per receiver position and average the estimation error to obtain the mean squared error (MSE) on ϕ_i and α_i, averaged over the $K = 4$ LEDs, and z_U for that position, i.e.

$$MSE_\phi = \frac{1}{K}\sum_{i=1}^{K} E[(\phi_i - \hat{\phi}_i)^2]$$

$$MSE_\alpha = \frac{1}{K}\sum_{i=1}^{K} E[(\alpha_i - \hat{\alpha}_i)^2]$$

$$MSE_{z_U} = E[(z_U - \hat{z}_U)^2]. \tag{22}$$

In Fig. 3, the root of the MSE (rMSE) on the incident angle ϕ_i, the polar angle α_i and the height z_U is shown as function of the position (x_U, y_U) of the receiver in the area. The red dots indicate the positions of the LEDs. As can be observed, the coarse estimation step returns an estimate for ϕ_i with an average error of less than 8 degrees, while the average error on α_i is smaller, except just below the LEDs, where the coarse estimator returns an estimate for α_i with a large error. However, below a LED, the polar angle α_i of that LED is not defined, which explains this large error. Further, in the centre cross section of the area, the height z_U can be estimated with an accuracy of 10-20 cm, while for a large part of the area, the error equals 50 cm. This latter error corresponds to the choice of the initial estimate $\hat{z}_U^{(0)} = -1.5$ m, i.e. the triangulation algorithm is not able to return an estimate of z_U due to the limitations of the coarse estimation algorithm. The center cross section coincides with the area within which the incident angle can be estimated with an accuracy of 1-2 degrees or better (see Fig. 3(a)). Hence, we can conclude that the triangulation algorithm is able to deliver an accurate estimate of the height z_U only if $rMSE_\phi < 1 - 2$ degrees. From these results, it is clear that the proposed simple coarse estimator will not be able to estimate the position of the receiver with centimetre accuracy for all positions in the area, although the estimates of ϕ_i and α_i will turn out to be satisfactory as an initial estimate.

In the next step, we feed the initial estimates to the ML estimator from Section III-B, without iterating the algorithm. The results are shown in Fig. 4. As can be observed, the ML estimator is able to strongly reduce the estimation errors on ϕ_i and α_i. Only just below a LED, the estimation error on α_i stays

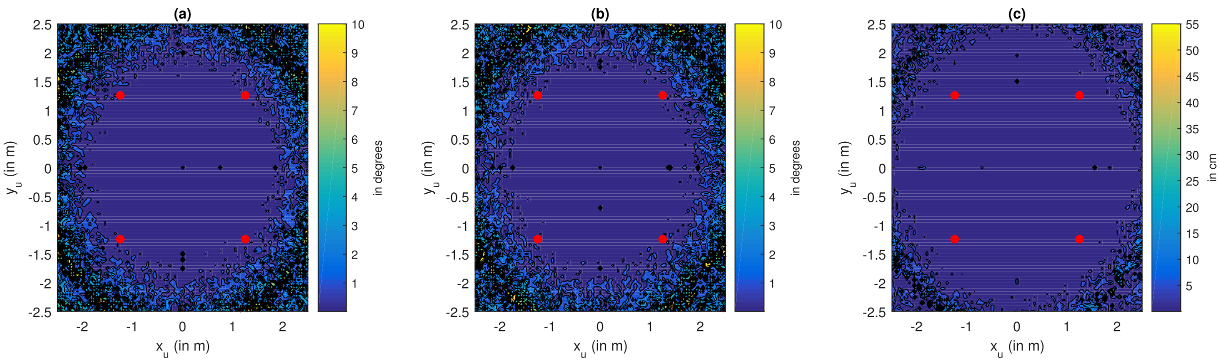

Fig. 5. rMSE of the iterative algorithm for (a) ϕ_i (b) α_i (c) z_U as function of the position of the receiver in the room, for $A_i = 1$ W, $T = 0.01$ s, $M = 8$, $x_{\max} = y_{\max} = 5$ m, $R = 2.5$ m, $h = 2$ m, maxiterations $= 10$.

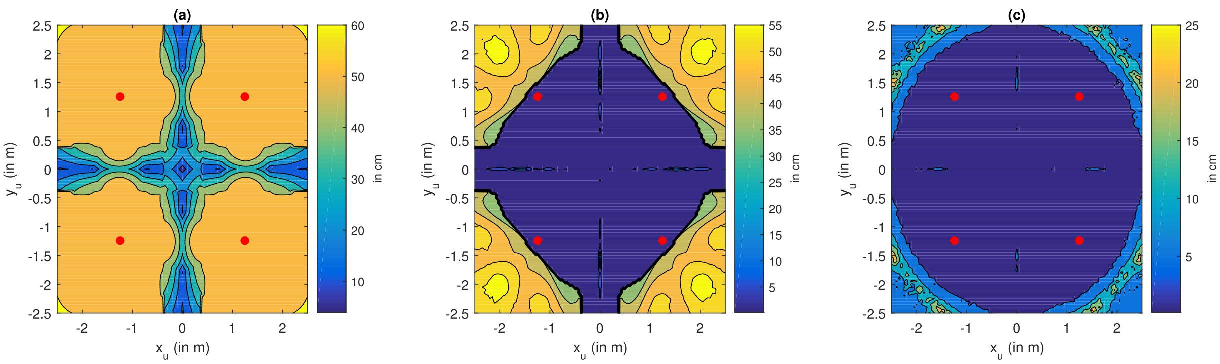

Fig. 6. rMSE on the receiver position for (a) coarse estimation (b) ML without iteration (c) iterative algorithm, as function of the position of the receiver in the room, for $A_i = 1$ W, $T = 0.01$ s, $M = 8$, $x_{\max} = y_{\max} = 5$ m, $R = 2.5$ m, $h = 2$ m.

large, due to the undefined α_i of that LED. Also the estimate of the height z_U strongly improves: in a large central part of the area, where the receiver is surrounded by LEDs, the estimation error on z_U drops below 5 cm. However, in the corners of the area, the estimation error on z_U remains large. This can be explained as follows. Note that the coarse estimator for ϕ_i can only deliver estimates when $\phi_i < 0.9\phi_{\max}$. In our example, $\phi_{\max} = \text{atan}(1.5)$, which implies that we can only estimate ϕ_i within a radius $d = (z_{S,i} - z_U)\tan(0.9\phi_{\max}) = 2.44$ m, assuming $z_{S,i} - z_U = 2$ m. The ML algorithm, which takes as input the estimates of the angles ϕ_i and α_i, and the height z_U, is able to accurately estimate the AOA of a LED, even if the initial estimate of z_U is unreliable, as long as the position approximately lies within a distance d of at least two LEDs. This corresponds to the blue central area in Fig. 4(a). However, outside this central area, the ML algorithm can only accurately estimate the AOA for the nearest LED, but not for the LEDs further away. As a result, the triangulation algorithm is not able to estimate the height z_U accurately, although the situation is improved compared to Fig. 3(c), due to the more accurate estimate of ϕ_i for the nearest LED.

To improve the convergence, we iterate our algorithm until the difference between two successive estimates of the position is sufficiently small (i.e. $||\hat{\boldsymbol{\rho}}^{(\ell)} - \hat{\boldsymbol{\rho}}^{(\ell-1)}|| < 1$ mm) or a maximum number of iterations is reached ($maxiterations = 10$). The results are shown in Fig. 5: the error on ϕ_i and α_i is very small for the largest part of the area and also the estimation error on z_U is less than 5 cm for the majority of the area. Only in the corners of the area, the errors can be larger. Compared to Fig. 4, the errors of α_i in the corners of Fig. 5 are increased. This can be explained as follows. In the corners, the initial error on the height z_U is large. As this height serves as an input to the ML step, the error on the height will push the ML estimates of the AOA away from the true AOA. The ML algorithm is able to correct for this deviation for the nearest LED, but not for the LEDs further away, resulting in an increase of the rMSE on α_i in the corners compared to the previous iteration. In the subsequent triangulation phase, the accuracy of the AOA for the nearest LED will result in a more accurate estimate of the height. Hence, in the different steps of the algorithm, accuracy of the AOA and accuracy on the height are constantly interchanged.

Finally, to compare the accuracy of the position estimate in the different steps, we show the rMSE on the position, i.e.

$$rMSE = \sqrt{E[(x_U - \hat{x}_U)^2 + (y_U - \hat{y}_U)^2 + (z_U - \hat{z}_U)^2]}, \qquad (23)$$

in Fig. 6. The results show that with the coarse estimator (Fig. 6(a)), 3D centimetre accuracy, i.e. a positioning error of less than 10 cm, can only be obtained in the centre cross section of the area, while with the non-iterated ML algorithm (Fig. 6(b)), centimetre accuracy can be achieved for a large central part of the area. However, when iterat-

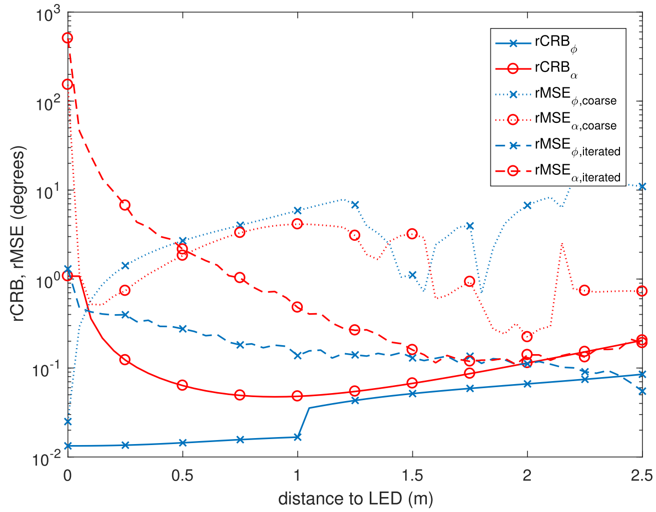

Fig. 7. Comparison of the rCRB and rMSE of the incident angle ϕ_i and polar angle α_i as function of the horizontal distance of the LED to the receiver for $A_i = 1$ W, $T = 0.01$ s, $M = 8$, $x_{\max} = y_{\max} = 5$ m, $R = 2.5$ m, $h = 2$ m, maxiterations = 10.

ing the ML algorithm (Fig. 6(c)), 3D centimetre positioning accuracy is attained in the whole area, except for some isolated positions in the corners, where the positioning error is of the order of 20 cm. To obtain this accuracy, the algorithm only needed less than 3-4 iterations for the central area, while more iterations were needed for the edges of the area. This could be expected: with a good initial estimate, the practical implementation of the ML algorithm converges well to the true AOA, and thus the true position, so that iterating more would only result in diminishing return. On the other hand, in the edges of the area, the initial position estimate can be far from the true position. As the ML algorithm is insufficiently able to correct large errors in the estimated height z_U – although the estimates of ϕ_i and α_i may be accurate – convergence of the estimated height must be obtained through the triangulation step. In our simulations, we found that in the first iterations, the estimated height only improves with 5-15 cm per iteration depending on the accuracy of the initial estimates of ϕ_i and α_i in that iteration, and the convergence speed reduces when the estimated height gets closer to the true height, i.e. after a few iterations. Hence, if the initial, coarse estimate of the height is 50 cm away from the true height, it can take 10 iterations or more for the position estimate to converge.

To evaluate the performance of the estimator for the AOA, we compare the rMSE on the AOA of the coarse estimator and the iterative algorithm with the root of the Cramer Rao bound (rCRB), as derived in [21]. For the iterative algorithm, we consider the case where four LEDs are arranged in a square grid with spacing 2.5 m, and are at a height $h = 2$ m above the receiver. The rMSE shown in Fig. 7 is the rMSE for one LED, i.e. it is not averaged over the four LEDs. As can be observed, the rMSE of the coarse estimator is considerably higher than the theoretical lower bound. This could be expected as the initial estimator only roughly estimates the AOA. Further, the figure demonstrates that, as expected, the rMSE of the AOA is lower than for the coarse estimator, and that for

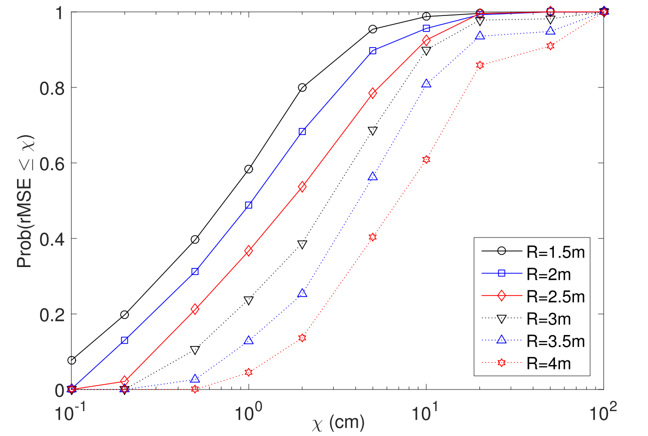

Fig. 8. Cumulative distribution function of the rMSE being smaller than a value χ (cm) for different spacings R between the LEDs, for $A_i = 1$ W, $T = 0.01$ s, $M = 8$, $x_{\max} = y_{\max} = 5$ m, $h = 2$ m.

some AOAs, it even reaches the rCRB. Hence, it can be concluded that the proposed iterative estimator is able to accurately estimate the AOA.

The effect of the spacing R between the LEDs is investigated in Fig. 8. In this figure, the cumulative distribution function of the rMSE being smaller than χ cm is shown. This cumulative distribution function gives an indication of the fraction of the positions for which the position can be estimated with an accuracy of χ cm or better. As can be observed, the positioning accuracy improves when the LEDs are closer to the centre of the area, i.e. when R reduces. This can be explained as follows. When the LEDs are closer to the centre of the area, the distance between the LED and the receiver placed in the opposite corner of the area is smaller. Because of this smaller distance between the LED and the receiver, the signal from this LED will be less attenuated by the channel. Moreover, the incident angle ϕ_i for that LED will be smaller, and therefore the coarse estimator can estimate the AOAs with a higher reliability. At the same time, the distance between the LED and the nearest corner increases, implying the incident angle between the LED and the receiver in this nearest corner increases. Consequently, if R is too small, for none of the LEDs the incident angle can be estimated in a reliable way, implying the initial, coarse position estimate is far from the real position and the iterative ML algorithm fails to converge. In our example, this occurred when $R < 1.5$ m. When $R = 1.5$ m, in 98.8% of the positions in the considered area, a 3D positioning accuracy of 10 cm or better is obtained.

The effect of the height z_U of the receiver and the initial estimate $\hat{z}_U^{(0)}$, in case the triangulation algorithm is not able to return an estimate for z_U, is shown in Fig. 9. As can be observed, for a given height z_U, the estimation accuracy improves when the initial estimate $\hat{z}_U^{(0)}$ for the height is closer to the true height. This could be expected, as when the initial estimate for z_U is closer to z_U, the iterative ML algorithm will converge better. When comparing the accuracy for different heights z_U, we can distinguish two effects. For small values of χ, we observe that the number of positions with an accuracy better than χ cm slightly increases when $|z_U|$ increases. This

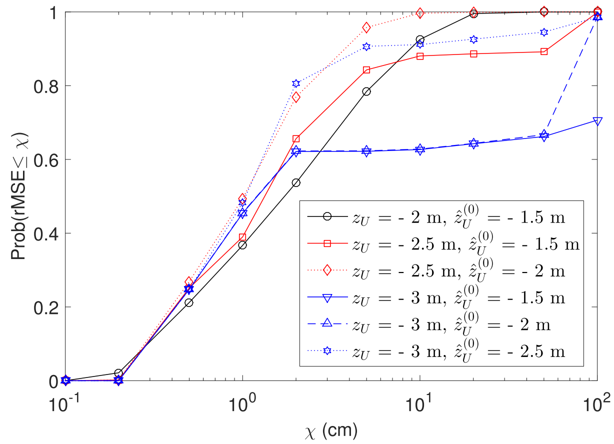

Fig. 9. Cumulative distribution function of the rMSE being smaller than a value χ (cm) for different heights z_U and initial estimates $\hat{z}_U^{(0)}$ for the height, for $A_i = 1$ W, $T = 0.01$ s, $M = 8$, $x_{\max} = y_{\max} = 5$ m, $R = 2.5$ m.

can be explained as when the receiver is further away from the ceiling while it is at the same (x_U, y_U) position, the incident angle ϕ_i reduces, implying the coarse estimator for ϕ_i can deliver reliable estimates for ϕ_i for more positions in the room, resulting in a better accuracy for a larger number of positions. On the other hand, we also observe at higher χ that the accuracy degrades when $|z_U|$ increases. This effect can be attributed to the positions in the area for which the incident angle can not be estimated in a reliable way by the coarse estimator. As the channel attenuation increases when $|z_U|$ grows, the smaller RSS values will cause the iterative ML estimator to have a worse performance for these positions, as the noise contribution will be relatively larger. From this figure, we can conclude that the proposed estimator is still able to estimate the receiver position with an accuracy of 10 cm or better in more than 90% of the positions when the vertical distance $|z_U|$ between the ceiling and the receiver grows.

V. Conclusions

In this paper, we propose a practical estimator for 3D positioning that extracts the AOA from the received signal by comparing the relative differences between the received signal strengths and computes the position of the receiver through triangulation. Hence, the algorithm does not require the knowledge of the transmitted optical power. The algorithm is based on the ML estimator. As the practical implementation of the ML algorithm has convergence problems when the initial position estimate is far from the true position, an initial estimator that delivers the AOA and the vertical distance between the LEDs and the receiver is required. We propose a low-complexity, coarse initial estimator that returns the AOA with sufficient accuracy. Combining the coarse estimator with the ML estimator, we obtain centimetre accuracy, i.e. an average positioning error of 10 cm or better, for all positions that are surrounded by the LEDs. However, for the positions that are not surrounded by LEDs, i.e. in the corners of the area, an accurate initial estimate of the vertical distance between the LEDs and the receiver can not be obtained with the coarse estimator. As a result, the practical implementation of the ML algorithm can not return accurate estimates of the position. To solve this problem, we consider an iterative algorithm, where the position estimate obtained with the triangulation is used to update the initial estimates for the AOA and the vertical distance estimate for the next iteration. We iterate until convergence is reached or until a maximum number of iterations is reached. Our simulation results show that the iterative algorithm is able to achieve centimetre accuracy for the majority of the positions in the area, with some outliers of the order of 20 cm in isolated positions. The resulting positioning accuracy is of the same order as other VLP systems, and although the complexity of the proposed estimator is higher than e.g. for the RSS-based approach, the VLP system solves practical issues encountered in these RSS-based system, i.e. the considered aperture-based receiver does not require the knowledge of the transmitted optical power, which is hard to obtain in practice.

References

[1] J. Armstrong, Y. Sekercioglu, and A. Neild, “Visible light positioning: A roadmap for international standardization,” *IEEE Commun. Mag.*, vol. 51, no. 12, pp. 68–73, Dec. 2013.

[2] M. Biagi, S. Pergoloni, and A.-M. Vegni, “LAST: A framework to localize, access, schedule, and transmit in indoor VLC systems,” *J. Lightw. Technol.*, vol. 33, no. 9, pp. 1872–1887, May 1, 2015.

[3] S. Hann, J.-H. Kim, S.-Y. Jung, and C.-S. Park, “White LED ceiling lights positioning systems for optical wireless indoor applications,” in *Proc. ECOC*, Torino, Italy, Sep. 2010, pp. 1–3.

[4] S.-Y. Jung, S. Hann, and C.-S. Park, “TDOA-based optical wireless indoor localization using LED ceiling lamps,” *IEEE Trans. Consum. Electron.*, vol. 57, no. 4, pp. 1592–1597, Nov. 2011.

[5] K. Panta and J. Armstrong, “Indoor localisation using white LEDs,” *Electron. Lett.*, vol. 48, no. 4, pp. 228–230, Feb. 2012.

[6] A. Arafa, X. Jin, and R. Klukas, “Wireless indoor optical positioning with a differential photosensor,” *IEEE Photon. Technol. Lett.*, vol. 32, no. 14, pp. 1027–1029, Jun. 15, 2012.

[7] S.-Y. Jung, S. Hann, S. Park, and C.-S. Park, “Optical wireless indoor positioning system using light emitting diode ceiling lights,” *Microw. Opt. Technol. Lett.*, vol. 54, no. 7, pp. 1622–1626, Jul. 2012.

[8] M. Rahaim, G. B. Prince, and T. D. C. Little, “State estimation and motion tracking for spatially diverse VLC networks,” in *Proc. Globecom Workshops*, Anaheim, CA, USA, Dec. 2012, pp. 1249–1253.

[9] H.-S. Kim, D.-R. Kim, S.-H. Yang, Y.-H. Son, and S.-K. Han, “An indoor visible light communication positioning system using a RF carrier allocation technique,” *J. Lightw. Technol.*, vol. 31, no. 1, pp. 134–144, Jan. 1, 2013.

[10] U. Nadeem, N. U. Hassan, M. A. Pasha, and C. Yuen, “Highly accurate 3D wireless indoor positioning system using white LED lights,” *Electron. Lett.*, vol. 50, no. 11, pp. 828–830, May 2014.

[11] G. Kail, P. Maechler, N. Preyss, and A. Burg, “Robust asynchronous indoor localization using LED lighting,” in *Proc. IEEE Int. Conf. Acoust., Speech Signal Process. (ICASSP)*, Florence, Italy, May 2014, pp. 1866–1870.

[12] S.-H. Yang, H.-S. Kim, Y.-H. Son, and S.-K. Han, “Three-dimensional visible light indoor localization using AOA and RSS with multiple optical receivers,” *J. Lightw. Technol.*, vol. 32, no. 14, pp. 2480–2485, Jul. 15, 2014.

[13] M. Yasir, S.-W. Ho, and B. N. Vellambi, “Indoor positioning system using visible light and accelerometer,” *J. Lightw. Technol.*, vol. 32, no. 19, pp. 3306–3316, Oct. 1, 2014.

[14] Y. U. Lee and S.-M. Lee, “Random distributed angle-of-arrival parameter estimation technique for visible light positioning,” in *Proc. Int. Conf. Telecommun. Signal Process. (TSP)*, Prague, Czech Republic, Jul. 2015, pp. 467–471.

[15] M. F. Keskin and S. Gezici, “Comparative theoretical analysis of distance estimation in visible light positioning systems,” *J. Lightw. Technol.*, vol. 34, no. 3, pp. 854–865, Feb. 1, 2016.

[16] D. Li, C. Gong, and Z. Xu, “A RSSI-based indoor visible light positioning approach,” in *Proc. 10th Int. Symp. Commun. Syst., Netw. Digit. Signal Process. (CSNDSP)*, Prague, Czech Republic, Jul. 2016, pp. 1–6.

[17] Q.-L. Li, J.-Y. Wang, T. Huang, and Y. Wang, "Three-dimensional indoor visible light positioning system with a single transmitter and a single tilted receiver," *Opt. Eng.*, vol. 55, no. 10, p. 106103, Oct. 2016.

[18] T. Q. Wang, C. He, and J. Armstrong, "Angular diversity for indoor MIMO optical wireless communications," in *Proc. IEEE Int. Conf. Commun. (ICC)*, London, U.K., Jun. 2015, pp. 5066–5071.

[19] H. Steendam, T. Q. Wang, and J. Armstrong, "Cramer-Rao bound for indoor visible light positioning using an aperture-based angular-diversity receiver," in *Proc. IEEE Int. Conf. Commun. (ICC)*, Kuala Lumpur, Malaysia, May 2016, pp. 1–6.

[20] H. Steendam, T. Q. Wang, and J. Armstrong, "Theoretical lower bound for indoor visible light positioning using received signal strength measurements and an aperture-based receiver," *J. Lightw. Technol.*, vol. 35, no. 2, pp. 309–319, Jan. 15, 2017.

[21] H. Steendam, T. Q. Wang, and J. Armstrong, "Cramer-Rao bound for AOA-based VLP with an aperture-based receiver," in *Proc. IEEE Int. Conf. Commun. (ICC)*, Paris, France, May 2017, pp. 1–6.

[22] A. J. Lowery and J. Armstrong, "Orthogonal-frequency-division multiplexing for dispersion compensation of long-haul optical systems," *Opt. Exp.*, vol. 14, no. 6, pp. 2079–2084, 2006.

[23] J. M. Kahn and J. R. Barry, "Wireless infrared communications," *Proc. IEEE*, vol. 85, no. 2, pp. 265–298, Feb. 1997.

[24] H. L. Van Trees, *Detection Estimation and Modulation Theory*. New York, NY, USA: Wiley, 1968.

[25] L. Zeng *et al.*, "High data rate multiple input multiple output (MIMO) optical wireless communications using white led lighting," *IEEE J. Sel. Areas Commun.*, vol. 27, no. 9, pp. 1654–1662, Dec. 2009.

Heidi Steendam (M'01–SM'06) received the M.Sc. degree in electrical engineering and the Ph.D. degree in applied sciences from Ghent University, Ghent, Belgium, in 1995 and 2000, respectively.

Since 1995, she has been with the Digital Communications Research Group, Department of Telecommunications and Information Processing, Faculty of Engineering, Ghent University, first in the framework of various research projects, and since 2002 as a Professor in the area of digital communications. In 2015, she was a Visiting Professor at Monash University. She is the author of over 140 scientific papers in international journals and conference proceedings, for which several best paper awards were received. Her main research interests are in statistical communication theory, carrier and symbol synchronization, bandwidth-efficient modulation and coding, cognitive radio and cooperative networks, and positioning and visible light communication.

Since 2002, she has been an executive Committee Member of the IEEE Communications and Vehicular Technology Society Joint Chapter, Benelux Section, since 2012 the vice chair, and since 2017 the chair. She was active in various international conferences as technical program committee chair/member and session chair. In 2004 and 2011, she was the Conference Chair of the IEEE Symposium on Communications and Vehicular Technology, Benelux. From 2012 to 2017, she was an Associate Editor of the IEEE TRANSACTIONS ON COMMUNICATIONS and *EURASIP Journal on Wireless Communications and Networking*.